RSC Advances

PAPER

View Article Online
View Journal | View Issue

Cite this: RSC Adv., 2014, 4, 32335

Layer-by-layer deposition of antifouling coatings on stainless steel *via* catechol-amine reaction†

Li Qun Xu,[a] Dicky Pranantyo,[a] Jiankai Brent Liu,[a] Koon-Gee Neoh,[a] En-Tang Kang,*[a] Ying Xian Ng,[b] Serena Lay-Ming Teo*[b] and Guo Dong Fu[c]

Received 9th May 2014
Accepted 17th July 2014

DOI: 10.1039/c4ra04336g

www.rsc.org/advances

Stainless steel (SS) has been widely used as a construction material in maritime structures due to its good corrosion resistance. However, bacteria, algae, barnacles and other marine organisms can readily adhere to its surface in the process of biofouling, leading to serious structure failures and economic losses. In this work, layer-by-layer (LBL) deposition of functional polymer coatings on SS surface provides an alternative approach to combating marine fouling. The catechol-containing antifouling copolymer of dopamine methacrylamide and poly(ethylene glycol) methyl ether methacrylate (P(DMA-*co*-PEGMEMA)), and amino-rich branched poly(ethyleneimine) (PEI) were assembled sequentially on the SS surface *via* catechol-amine reaction in a LBL manner. The PEI/P(DMA-*co*-PEGMEMA) multiple bilayer-coated SS surfaces can effectively reduce the adhesion of bacteria and microalgae (microfouling), and settlement of barnacle cyprids (macrofouling), as compared to the pristine SS surface. The antifouling efficiencies of PEI/P(DMA-*co*-PEGMEMA) bilayer-coated SS surfaces were also significantly higher than that of the P(DMA-*co*-PEGMEMA) monolayer-coated SS surface.

Introduction

Stainless steel (SS) is of considerable importance because of its useful applications in the food industry and in biomedical devices and implants, arising from its durability and anticorrosion properties.[1–4] Stainless steel is also widely utilized in structures in marine and freshwater environments, including port installations, cooling water circuits, and vessels and their fittings.[5] However, stainless steel faces an unresolved problem of biofouling by a variety of microorganisms when exposed to humid and non-sterile environments.[5] Biofouling also presents a significant hygiene risk to the food and biomedical industries, resulting in device/structure failure and economic losses.[6,7] Thus, chemical treatment or modification of SS surfaces to confer the desired antifouling properties is essential. Strategies for surface functionalization, such as biomimetic coating,[8] salinization,[9] electrografting,[10] phosphate–metal oxide coordination,[11,12] autocatalytic plating and ion implantation,[13] have been developed to impart antifouling properties on SS surfaces.

Layer-by-layer (LBL) deposition technique has been proven to be an efficient and versatile means for depositing functional polymer coatings on surfaces.[14–18] The principles of LBL assembly mainly involve non-covalent interactions, such as electrostatic forces,[19] halogen bonding,[20] hydrogen bonding,[21] molecular recognition[22,23] and charge-transfer interaction.[24] However, the non-covalently assembled LBL films may not exhibit sufficient stability in harsh environments. Chemical,[25–28] thermal[29] and photo[30] routes have been employed to fabricate covalently bounded LBL films and enhance the stability of as-fabricated LBL films. Covalent crosslinking within the LBL films has also been achieved through various click reactions, such as copper(I)-catalyzed azide–alkyne cycloaddition (CuAAC),[31,32] thiol–ene chemistry,[33] azlactones–amine reaction[34,35] and reactive pentafluorophenyl (PFP) ester–amine reaction.[36] In our previous work,[32] the LBL technique and CuAAC have been utilized to fabricate robust multilayer functional polymer coatings for combating biofouling. On the other hand, amino moiety can spontaneously couple to catechol group *via* Michael addition/Schiff base reaction under basic condition,[37–40] leading to the formation of stable crosslinks within the LBL films.

In this work, catechol-containing poly(dopamine methacrylamide-*co*-polyethylene glycol methyl ether methacrylate), or P(DMA-*co*-PEGMEMA) random copolymers, were prepared *via* functionalization of the reactive PFP ester groups in poly(pentafluorophenyl methacrylate-*co*-PEGMEMA) (P(PFMA-*co*-PEGMEMA)) with dopamine hydrochloride (Scheme 1). Commercial poly(ethyleneimine) (PEI) was chosen for the LBL assembly, as the macromolecular mediating unit contains amine groups that are able to react with the catechol moieties.

[a]Department of Chemical & Biomolecular Engineering, National University of Singapore, Kent Ridge, 117576, Singapore. E-mail: cheket@nus.edu.sg
[b]Tropical Marine Science Institute, National University of Singapore, Kent Ridge, 119223, Singapore. E-mail: tmsteolm@nus.edu.sg
[c]School of Chemistry and Chemical Engineering, Southeast University, Jiangning District, Nanjing, Jiangsu Province, 211189, P. R. China

† Electronic supplementary information (ESI) available. See DOI: 10.1039/c4ra04336g

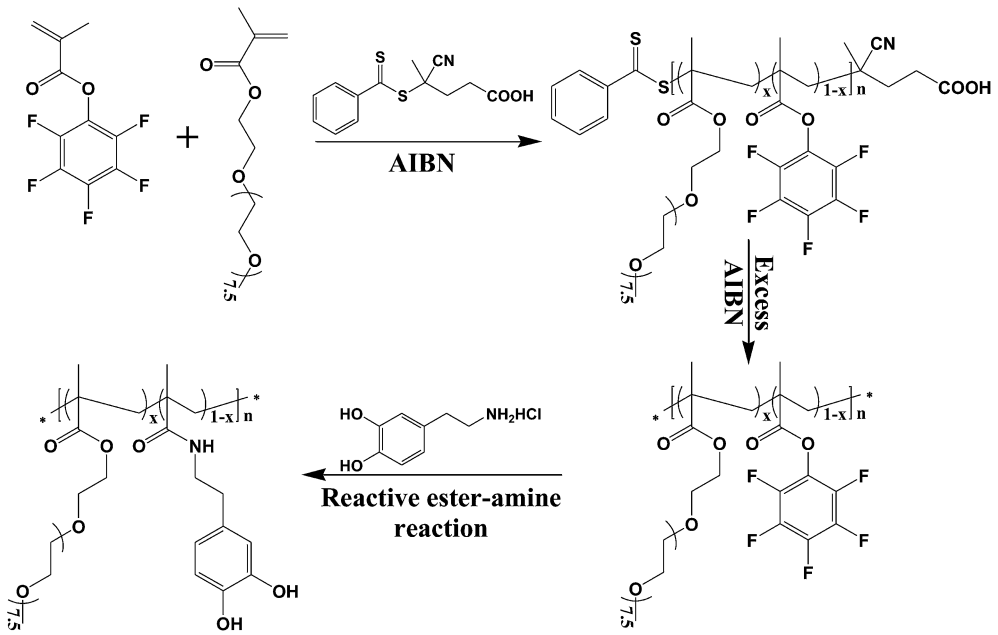

Scheme 1 Synthesis route of the P(DMA-*co*-PEGMEMA) copolymer.

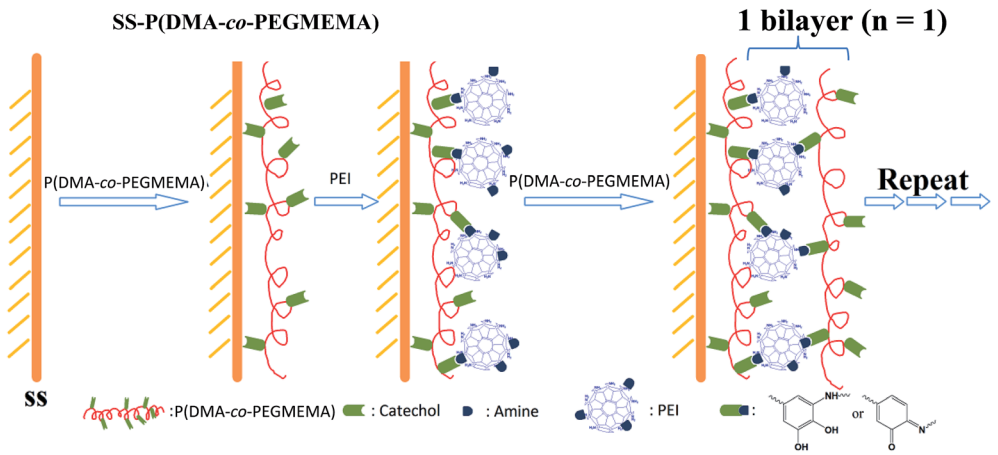

Scheme 2 LBL assembly of P(DMA-*co*-PEGMEMA) and PEI bilayers on the SS surface.

The P(DMA-*co*-PEGMEMA) copolymer was first coupled to the SS surface *via* coordination interaction of the catechol moieties to form the anchoring layer, followed by the deposition of the PEI and P(DMA-*co*-PEGMEMA) bilayers (Scheme 2). The antifouling efficiency of the resulting PEI/P(DMA-*co*-PEGMEMA) multilayer coatings was assayed with the adhesion of bacteria (*Pseudomonas* sp.) and microalgae (*Amphora coffeaeformis*), and settlement of barnacle cyprids (*Amphibalanus* (= *Balanus*) *Amphitrite*).

Experimental section

Materials

Stainless steel (SS) foils (AISI type 304, Fe/Cr18/Ni10, 0.05 mm thick) were purchased from Goodfellow Ltd., Cambridge, UK. 4-Cyano-4-(phenylcarbonothioylthio)pentanoic acid (CPA, 97%), dopamine hydrochloride, poly(ethylene glycol) methyl ether methacrylate (PEGMEMA, $M_n \sim 475$), branched poly(ethyleneimine) (PEI, $M_w \sim 25\,000$, $M_n \sim 10\,000$) and 2,2′-azoisobutyronitrile (AIBN, 98%) were purchased from Sigma-Aldrich Chemical Co. All other regents were purchased from Sigma-Aldrich or Merck Chem. Co., and were used without further purification. Pentafluorophenyl methacrylate (PFMA) was synthesized according to the method reported in the literature.[41]

Synthesis of poly(PFMA-*co*-PEGMEMA) (P(PFMA-*co*-PEGMEMA)) random copolymers

CPA (200.0 mg, 0.72 mmol), AIBN (23.5 mg, 0.14 mmol), PEGMEMA (8.3 mL, 17.9 mmol) and PFMA (0.65 mL, 3.6 mmol) were dissolved in 8 mL of 1,4-dioxane, under magnetic stirring, in a

25 mL round-bottom flask. The reaction mixture was degassed with argon for 30 min. The flask was sealed and kept in a 70 °C oil bath under stirring for 12 h. The reaction mixture was then cooled in an ice bath, diluted with 10 mL of THF, and precipitated into 200 mL of cold hexane. After pouring away the supernatant, the precipitate was dried by exposure to air, dissolved in doubly-distilled water, and dialyzed with doubly-distilled water for 3 days. The resulting solution was freeze-dried. The copolymer obtained is referred to as the P(PFMA-*co*-PEGMEMA)1 copolymer. The resulting copolymer samples prepared from [CDP] : [AIBN] : [PEGMEMA] : [PFMA] molar feed ratios of 1 : 0.2 : 37.5 : 7.5 and 1 : 0.2 : 50 : 10 are referred to as the P(PFMA-*co*-PEGMEMA)2 and P(PFMA-*co*-PEGMEMA)3 copolymers, respectively.

Synthesis of poly(dopamine methacrylamide-*co*-PEGMEMA) (P(DMA-*co*-PEGMEMA)) random copolymers

The removal of the dithioester is crucial in preventing the formation of disulfide coupling bond, which may occur during post-functionalization of the polymer precursor.[42] The dithioester of the P(PFMA-*co*-PEGMEMA) copolymers was removed with 30 equivalent of AIBN in tetrahydrofuran (THF) at 65 °C until the red color had faded. The resulting P(PFMA-*co*-PEGMEMA) copolymers were isolated by precipitation into hexane. The crude product was re-dissolved in THF. The re-dissolution and precipitation processes were repeated three times.

For the synthesis of P(DMA-*co*-PEGMEMA) copolymer, P(PFMA-*co*-PEGMEMA)1 (5.0 g) and dopamine hydrochloride (0.80 g, 4.2 mmol) were dissolved in 20 mL of DMF in a 50 mL round bottom flask. Excess dopamine hydrochloride was used to ensure the complete conversion of the reactive pentafluorophenyl (PFP) ester groups into catechol-based amide moieties. Triethylamine (0.59 mL, 4.2 mmol) was added into the solution and the reaction mixture was stirred at 50 °C under an argon atmosphere. After 24 h of stirring, the reaction mixture was cooled down to room temperature and dialyzed with doubly-distilled water for 3 days. About 3.9 g of the P(DMA-*co*-PEGMEMA) copolymer was obtained after lyophilization.

Assembly of PEI/P(DMA-*co*-PEGMEMA) multilayer coatings on SS surfaces

The SS foils were cut into 2 cm × 2 cm coupons and cleaned ultrasonically with doubly-distilled water, acetone and ethanol for 15 min each. The SS coupons were then rinsed thoroughly with doubly-distilled water and blown dry with compressed air. The clean SS coupons were activated by immersing in the piranha solution (H_2SO_4 (95–97%) : H_2O_2 (30%) = 3 : 1, v/v) for 30 min to generate a hydroxyl-enriched surface.

The SS coupons were immersed in the P(DMA-*co*-PEGMEMA) aqueous solution (20 mg mL^{-1}) at room temperature for 12 h. The resulting P(DMA-*co*-PEGMEMA) monolayer-anchored SS substrate (SS-P(DMA-*co*-PEGMEMA)) was then exposed to the PEI aqueous solution (20 mg mL^{-1}) for 30 min, followed by washing with doubly-distilled water to produce the SS-P(DMA-*co*-PEGMEMA)/PEI substrate. Subsequently, the substrate was immersed into the P(DMA-*co*-PEGMEMA) aqueous solution (20 mg mL^{-1}) for 30 min, and then rinsed with doubly-distilled water 3 times and dried with compressed air to obtain the first PEI/P(DMA-*co*-PEGMEMA) bilayers coating on the SS surface. The multiple bilayers-coated SS substrate obtained from *n*-times of alternate immersion into PEI and P(DMA-*co*-PEGMEMA) solutions are denoted as the SS-(PEI/P(DMA-*co*-PEGMEMA))$_n$ substrate (Scheme 2).

Bacteria adhesion on the SS-(PEI/P(DMA-*co*-PEGMEMA))$_n$ substrates

Marine bacteria, *Pseudomonas* sp. (NCIMB 2021), were used to evaluate the antibacterial adhesion characteristics of the polymer multilayer coatings. *Pseudomonas* sp. was cultured in a nutrient-rich artificial seawater medium containing 5 g L^{-1} of peptone from the enzymatic digest of gelatin and 3 g L^{-1} of beef extract at a pH of 6.8.[43] After incubation at 37 °C for 2 days, the bacterial suspension was centrifuged at 2700 rpm for 10 min. After removal of the supernatant and washing twice with artificial seawater, the bacterial cells were resuspended in artificial seawater at a concentration of 10^8 cells per mL. Each substrate was then immersed in 1 mL of bacterial suspension in a 24-well plate under static condition at 37 °C for 4 h. Quantification of bacteria adhesion on the pristine and polymer-coated SS substrates was determined using the spread plate method. The bacteria suspension in each well was gently removed by aspiration using a pipette, and 1 mL of artificial seawater was slowly added to each well along the wall. The artificial seawater was then gently pipetted away. After washing with artificial seawater for three times, the substrates were put into 3 mL of artificial seawater and subjected to ultrasonication for 7 min, and followed by vortexing for 20 s to release the cells. The bacterial solution was then serially diluted, spread on agar plate, and cultured overnight to quantify the number of bacterial cells. All experiments were performed in triplicate with three samples and the mean values were calculated. The number of adherent bacterial cells was expressed as cells per cm^2 of substrate surface.

Amphora adhesion on the SS-(PEI/P(DMA-*co*-PEGMEMA))$_n$ substrates

Amphora coffeaeformis (UTEX reference number B2080) was cultured in F/2 medium in tissue culture flasks in an environmental culture chamber at 24 °C with a 12 h/12 h light/dark cycle.[44] The *Amphora* cells can be used when the tissue culture flask surface is confluent. After that, the *Amphora* cells were removed from the surface of the tissue culture flask *via* gentle scraping. The *Amphora* clumps were subsequently broken up by continuous pipetting and filtering through a 35 μm nitex mesh. The total number of cells collected per milliliter was determined using a hemocytometer. Finally, the *Amphora* cells were diluted with 30‰ salinity, filtered (0.22 μm filter) seawater to a concentration of 10^5 cells per mL prior to use.

The pristine and polymer-coated SS substrates were cut into coupons of about 1 cm × 1 cm in size. The coupons were then placed in a 24-well plate (Nalge, Nunc International, Rochester,

NY), and covered with 0.5 mL of *Amphora* suspension (10^5 cells per mL) at room temperature for 24 h. The coupons were then washed three times with doubly-distilled water to remove any non-adhered or loosely adhered *Amphora* cells. The rinsing procedures for *Amphora* adhesion assay were similar to those for bacteria adhesion assay, with all the artificial seawater roles being replaced by doubly-distilled water. The adhered *Amphora* cells on the coupons were viewed with a Nikon Eclipse Ti microscope, equipped with an excitation filter of 535 nm and an emission filter of 617 nm.

Quantification of the adhered *Amphora* cells was carried out by the fluorescence technique. Briefly, after washing with doubly-distilled water as described above, the substrates were put into 2 mL of 30‰ salinity, filtered seawater and subjected to ultrasonication for 10 min. After that, 200 μL aliquots of the *Amphora* suspension were transferred to a 96-well microplate (PS F-bottom from Greiner Bio-One). The fluorescence intensity of each well at 690 nm was then measured at an excitation wavelength of 440 nm on a *Tecan Infinite M200* Microplate Reader. The fluorescence intensity of 30‰ salinity, filtered seawater was chosen as the blank. All experiments were performed in triplicate with three samples and the mean values were calculated. The results were expressed as percentages relative to the cell number obtained from the pristine SS surface.

Barnacle cyprid settlement on the SS-(PEI/P(DMA-*co*-PEGMEMA))$_n$ substrates

The culturing of cypris larvae from adult barnacles (*Balanus amphitrite*) was carried out following the published method.[45] For the settlement assay, a 2 cm × 2 cm of pristine or polymer-coated SS substrate was placed on a watch glass with a double-sided adhesive taped on the bottom. The substrate was gently pressed to form a concave trough, into which 0.5 mL of cyprid suspension containing approximately 30 larvae was introduced to form a round wetting spot. The settlement was allowed to proceed in the dark at room temperature for 24 h. The settled cyprids were counted against their total number under a microscope. The dead fraction of cyprids can be distinguished *via* the detachment of their legs from the body when observed in a 24 h settlement assay, while the settled cyprids can be found cemented headfirst to the substrate or metamorphosed into a juvenile barnacle with developed calcareous plates to surround themselves. Each settlement test was performed in triplicate to obtain a reliable mean result.

Characterization

The chemical structure of obtained polymers was characterized by ^{1}H NMR spectroscopy on a Bruker DRX 400 MHz spectrometer. Gel permeation chromatography (GPC) was performed on a Waters GPC system, equipped with a Waters 1515 isocratic HPLC pump, a Waters 717 plus Autosampler injector, a Waters 2414 refractive index detector and a PLgel 10 μm Mixed-B column (Agilent Technologies, S/N 10M-MB-D7-9K8), using THF as the eluent at a flow rate of 1.0 mL min^{-1} at 35 °C. The calibration curve was generated using polystyrene molecular weight standards. X-ray photoelectron spectroscopy (XPS) measurements were carried out on a Kratos AXIS Ultra HSA spectrometer equipped with a monochromatized AlKα X-ray source (1468.71 eV photons). FT-IR spectroscopy analysis was carried out on a Bio-Rad FTS-135 spectrophotometer. The UV-visible absorption spectra of PEI/P(DMA-*co*-PEGMEMA) bilayers-coated quartz slides were measured on a Shimadzu UV-3600 spectrophotometer equipped with a film holder. The thicknesses of PEI/P(DMA-*co*-PEGMEMA) multilayer coatings on quartz slides were determined by ellipsometry. The measurements were carried out on a variable angle spectroscopic ellipsometer (model VASE, J.A. Woollam Inc., Lincoln, NE) at incident angles of 65° and 75° in the wavelength range 500–1000 nm. Data were recorded and processed using the WVASE32 software package. The refractive index of the polymer layers was set as 1.45 for the Normal Fit.

Results and discussion

Synthesis of poly(dopamine methacrylamide-*co*-poly(ethylene glycol) methyl ether methacrylate) (P(DMA-*co*-PEGMEMA)) copolymers

The P(DMA-*co*-PEGMEMA) random copolymer was synthesized by a combination of reversible addition–fragmentation chain transfer (RAFT) polymerization and reactive ester–amine reaction. The detailed synthesis route, which consists of three consecutive steps, is shown in Scheme 1. The poly(pentafluorophenyl methacrylate-*co*-PEGMEMA) (P(PFMA-*co*-PEGMEMA)) random copolymers were synthesized *via* RAFT copolymerization of PEGMEMA and PFMA, using 4-cyano-4-(phenylcarbonothioylthio)pentanoic acid (CPA) as the chain transfer agent (CTA) and 2,2′-azoisobutyronitrile (AIBN) as the initiator. To maintain good solubility of the copolymer in the aqueous media, a high molar ratio (5 : 1) of the hydrophilic PEGMEMA units to hydrophobic PFMA units is required. The number-average molecular weights (M_n's), polydispersity index (PDI) and degrees of polymerization (DP's) of the corresponding P(PFMA-*co*-PEGMEMA) copolymers are summarized in Table S1 (ESI†). The GPC traces of P(PFMA-*co*-PEGMEMA) copolymers are shown in Fig. S1 (ESI†). The M_n's increase with the increase in monomers to CTA molar feed ratios, with the GPC traces shift to shorter elution times. However, the molecular weight distributions, corresponding to PDI, also increase with the increase in the monomers to CTA molar feed ratios. The P(PFMA-*co*-PEGMEMA)2 and P(PFMA-*co*-PEGMEMA)3 copolymers (Table S1†) exhibit a relatively high PDI (>1.4). Thus, the P(PFMA-*co*-PEGMEMA)1 copolymer with a lower molecular weight (PDI = 1.26) were used in this study.

Fig. 1a shows the ^{1}H and ^{19}F NMR spectra of P(PFMA-*co*-PEGMEMA)1 copolymer in DMSO-d_6. The chemical shifts at 4.03, 3.61, 3.52, 3.43 and 3.23 ppm are characteristic of the oligopoly(ethylene glycol) repeating units. Unfortunately, the characteristic chemical shifts of methyl and methylene protons on the backbone of PFMA are masked by those of the PEGMEMA repeating units. ^{19}F NMR analysis of the P(PFMA-*co*-PEGMEMA)1 copolymer was employed to verify the presence of PFMA repeating units. The ^{19}F NMR spectrum of the polymers

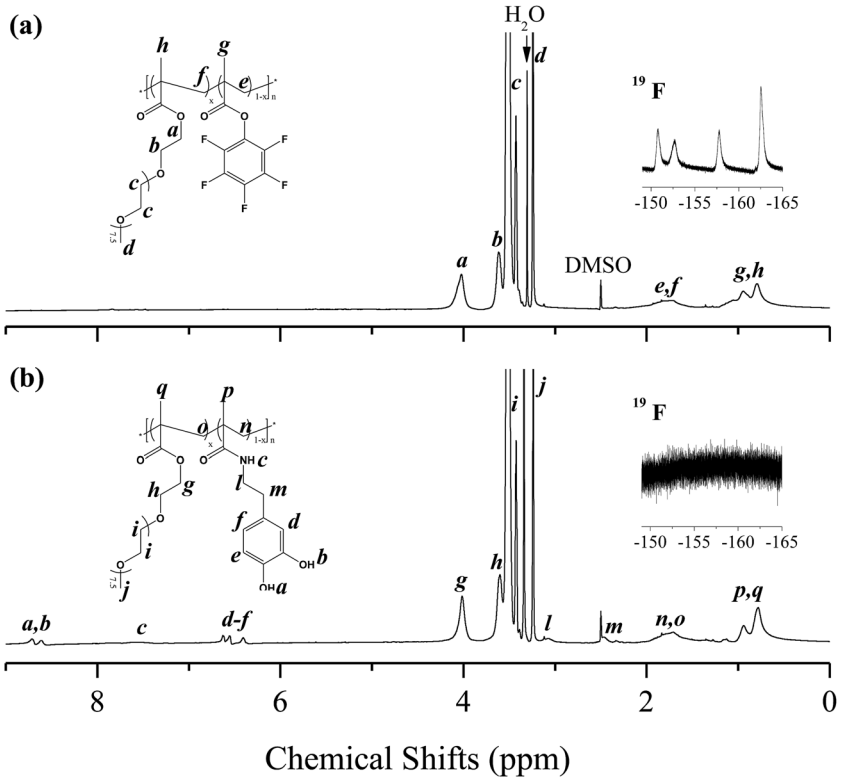

Fig. 1 ^{1}H and ^{19}F NMR spectra of the (a) P(PFMA-*co*-PEGMEMA)1 and (b) P(DMA-*co*-PEGMEMA) copolymers.

shows four board signals at −150.7, −152.7, −157.7 and −162.6 ppm. The chemical shifts for the *ortho*-fluorine atoms are split at −150.7 and −152.7 ppm, indicating the slight difference in the chemical environment of the two fluorine atoms due to the methyl group in the methacrylate backbone.[46] The FT-IR spectrum of P(PFMA-*co*-PEGMEMA)1 copolymer (Fig. S2†) confirms the successful copolymerization of PFMA. The FT-IR spectrum of P(PFMA-*co*-PEGMEMA)1 copolymer contains the characteristic absorption bands at around 1774 and 1522 cm^{-1}, which can be attributed to the vibration of reactive ester and pentafluorophenyl (PFP) group, respectively.[47]

The P(PFMA-*co*-PEGMEMA)1 copolymer was then modified by reactive ester–amine reaction with dopamine hydrochloride in the presence of triethylamine. Successful preparation of the P(DMA-*co*-PEGMEMA) copolymer was supported by the ^{1}H and ^{19}F NMR spectroscopy results of Fig. 1b. Post-functionalization of the P(PFMA-*co*-PEGMEMA)1 copolymer has led to the appearance of chemical shifts in the ranges of 8.56–8.81, 7.40–7.82 and 6.33–6.73 ppm, attributed to the respective hydroxyl, NH and aromatic protons of the catechol group,[48] and the disappearance of phenyl fluorine signals in the region of −150 to −163 ppm (inset of Fig. 1b). The P(DMA-*co*-PEGMEMA) copolymer was subsequently characterized by FT-IR spectroscopy (Fig. S2†). The barely discernible reactive ester group at about 1774 cm^{-1} and PFP moiety at 1522 cm^{-1} is consistent with the successful conversion of PFP groups to catechol groups. The M_n of the resulting P(DMA-*co*-PEGMEMA) copolymer is determined to be about 10 400 g mol^{-1} by GPC. The slight decrease in the M_n of the copolymers is probably due to the decrease in molecular weight per repeat unit of PDMA when converted from PFMA. The PDI of P(DMA-*co*-PEGMEMA) copolymer increases to 1.37, but remains in the controlled region (PDI < 1.4), suggesting the absence of side or cross-linking reaction during the post-functionalization reaction.

Assembly of poly(ethyleneimine)/P(DMA-*co*-PEGMEMA) (PEI/P(DMA-*co*-PEGMEMA)) multilayer coatings on stainless steel (SS) surfaces

The presence of PEI/P(DMA-*co*-PEGMEMA) coatings on the SS surfaces was ascertained by XPS analysis. The C 1s, O 1s, Cr 2p, Fe 2p and Ni 2p components with respective binding energies (BE's) at about 285, 530, 580, 710 and 860 eV are discernible in the XPS wide-scan spectrum of pristine SS surface (Fig. 2a). In comparison to the XPS wide-scan spectrum of pristine SS, the increase in intensity of C 1s signal and the decrease in the intensities of Cr 2p, Fe 2p and Ni 2p signals in the XPS wide-scan spectrum of SS-P(DMA-*co*-PEGMEMA) (Fig. 2b) indicate that the P(DMA-*co*-PEGMEMA) copolymer has been successfully anchored on the SS surface. After the introduction of PEI/P(DMA-*co*-PEGMEMA) multilayer coatings, the Cr 2p, Fe 2p and Ni 2p signals of SS substrates are no longer discernible in the XPS wide-scan spectra of SS-(PEI/P(DMA-*co*-PEGMEMA))$_n$ (n > 2), indicating that these multilayer coatings have good surface coverage. These results also suggest that the SS surfaces are covered by the PEI/P(DMA-*co*-PEGMEMA) multilayer coatings to a thickness greater than the probing depth of the XPS

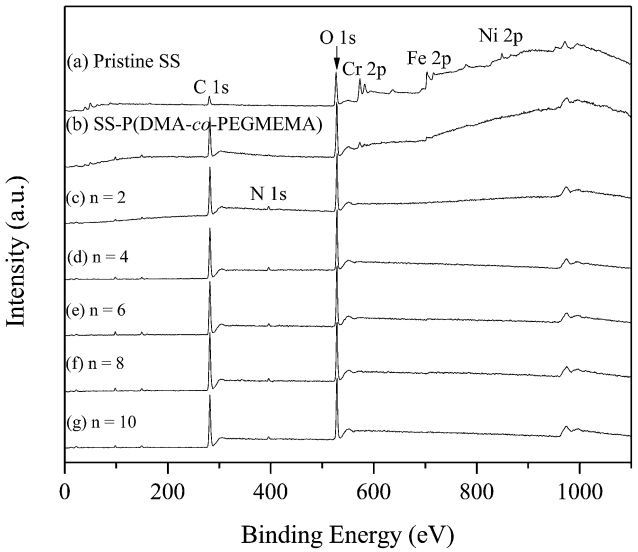

Fig. 2 XPS wide-scan spectra of the (a) pristine SS, (b) SS-P(DMA-*co*-PEGMEMA) and (c–g) SS-(PEI/P(DMA-*co*-PEGMEMA))$_n$ with $n = 2$, 4, 6, 8 and 10, respectively.

technique (~8 nm in an organic matrix[49]) after 2 bilayers. Fig. S3† shows the XPS C 1s core-level spectra of the pristine SS, SS-P(DMA-*co*-PEGMEMA) and SS-(PEI/P(DMA-*co*-PEGMEMA))$_n$ with $n = 2$, 4, 6, 8 and 10. The intensities of the C–O peak component have increased significantly after the deposition of PEI/P(DMA-*co*-PEGMEMA) bilayers. The line shapes of the XPS C 1s core-level spectra of SS-(PEI/P(DMA-*co*-PEGMEMA))$_n$ ($n = 2$, 4, 6, 8 and 10) are close to that of PEG-based polymers,[32] suggesting that the top layers of SS-(PEI/P(DMA-*co*-PEGMEMA))$_n$ substrates have been mainly covered by the PEG-based P(DMA-*co*-PEGMEMA) copolymers. The presence of hydrophilic PEI/P(DMA-*co*-PEGMEMA) coatings on the SS surfaces was also revealed by changes in static water contact angle. The water contact angle of pristine SS surface is about 78°, and it decreases to around 45° after deposition of 10 bilayers of hydrophilic PEI/P(DMA-*co*-PEGMEMA).

Since SS has a relatively rough surface, it is hard to monitor the growth of the multilayer polymer coatings by ellipsometry. An initial set of fabrication experiment to characterize the growth profiles of PEI/P(DMA-*co*-PEGMEMA) bilayers was performed on Quartz slides. Fig. 3a shows a plot of coating thickness (as determined by ellipsometry) as a function of the number of PEI/P(DMA-*co*-PEGMEMA) bilayers. As expected, the coating thickness increases with each bilayer deposited up to a value of about 191 nm at 10 bilayers. The multilayer coatings also show a linear increase in thickness, yielding a slope (corresponding to the bilayer thickness) of 19.1 nm per bilayer. In addition, the multilayer coatings absorb in the UV-visible region. Two absorption peaks at about 204 and 296 nm appear in the UV-visible adsorption spectra of the PEI/P(DMA-*co*-PEGMEMA) bilayer coated-Quartz slides (Fig. 3b). The absorbance at about 296 nm, characteristic of phenolic compounds,[50] increases almost linearly with the increase in number of PEI/P(DMA-*co*-PEGMEMA) bilayers (inset of Fig. 3b), confirming the uniform deposition of PEI/P(DMA-*co*-PEGMEMA) bilayers.

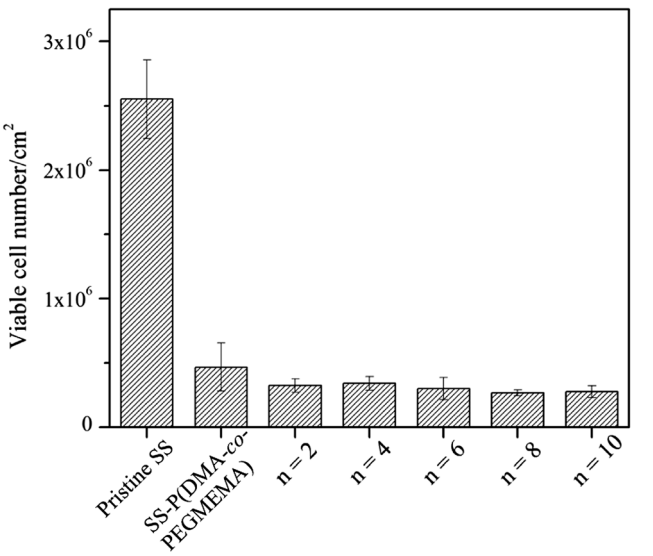

Fig. 4 Number of adhered *Pseudomonas* sp. cells per cm^2 of the pristine SS, SS-P(DMA-*co*-PEGMEMA) and SS-(PEI/P(DMA-*co*-PEGMEMA))$_n$ surfaces after exposure to bacterial suspension in artificial seawater (10^8 cells per mL) for 4 h. Error bars give the standard deviation obtained from three replicates.

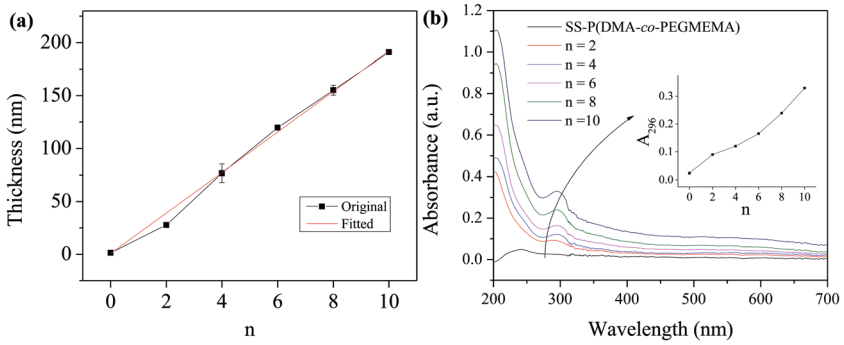

Fig. 3 (a) Coating thickness and (b) UV-visible absorption spectra of the PEI/P(DMA-*co*-PEGMEMA) bilayers on a Quartz slide as a function of bilayer number.

The stability of SS-(PEI/P(DMA-*co*-PEGMEMA))$_{10}$ coating on the SS surface was investigated in flowing filtered seawater medium of 30‰ salinity (Scheme S1†). The Cr 2p, Fe 2p and Ni 2p signals of SS substrates are still indiscernible in the XPS wide-scan spectra of SS-(PEI/P(DMA-*co*-PEGMEMA))$_{10}$ substrates after exposure to the flowing seawater at 23 °C for 30 days. Thus, the PEI/P(DMA-*co*-PEGMEMA) coatings are durable.

Bacteria adhesion on the SS-(PEI/P(DMA-*co*-PEGMEMA))$_n$ substrates

The PEG-based hydrated polymer coatings are known to repel proteins and extracellular polymeric substances secreted by the bacteria during the adhesion process.[51] The number of adhered bacteria on the pristine and PEG-based PEI/P(DMA-*co*-PEGMEMA) multilayers coated-SS surfaces was assayed quantitatively by the spread plate method. As shown in Fig. 4, there is a significant reduction in the number of adhered cells on the polymer coated-SS surfaces. The SS-P(DMA-*co*-PEGMEMA) and SS-(PEI/P(DMA-*co*-PEGMEMA))$_n$ (n = 2, 4, 6, 8, 10) surfaces reduce *Pseudomonas* sp. adhesion by ~82%, 87%, 87%, 88%, 89% and 89%, respectively, as compared to that of pristine SS surface. It has been reported that the anti-adhesive property of the polymer coated-SS surfaces is dependent on the thickness of the hydrophilic layer.[52] Thus, the ability of the SS-(PEI/P(DMA-*co*-PEGMEMA))$_n$ surface to inhibit *Pseudomonas* sp. adhesion approaches maximum after two PEI/P(DMA-*co*-PEGMEMA) bilayers.

Amphora adhesion on the SS-(PEI/P(DMA-*co*-PEGMEMA))$_n$ substrates

Amphora coffeaeformis is a common model organism for antifouling assay.[53] The anti-adhesion properties of the pristine and polymer-coated SS surfaces were revealed by the fluorescence microscopy images of adhered *Amphora* cells (Fig. 5). Significantly more *Amphora* cells attach on the pristine SS surface (Fig. 5a) than on the polymer-coated SS surfaces. Among the polymer-coated SS surfaces, the SS-(PEI/P(DMA-*co*-PEGMEMA))$_n$ (n = 2, 4, 6, 8) exhibit fewer adhered *Amphora* cells than that of the SS-P(DMA-*co*-PEGMEMA) surface. This phenomenon indicates that the former surfaces have better antifouling coverage,

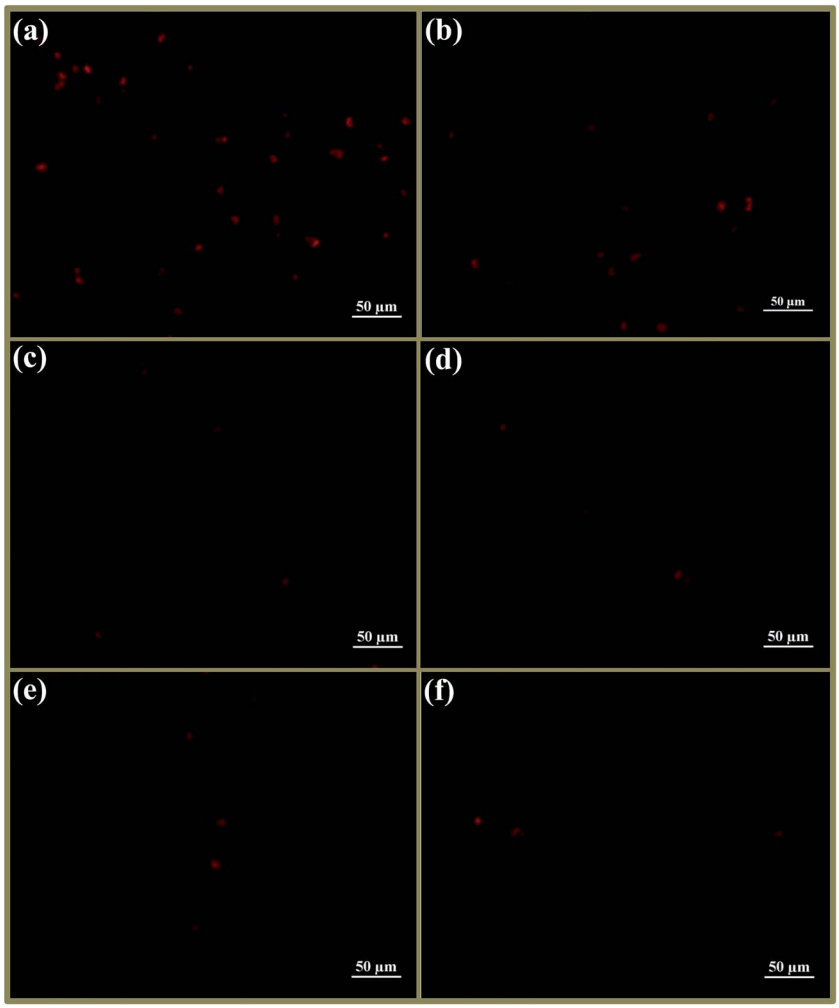

Fig. 5 Fluorescence microscopy images of the (a) pristine SS, (b) SS-P(DMA-*co*-PEGMEMA) and (c–f) SS-(PEI/P(DMA-*co*-PEGMEMA))$_n$ (n = 2, 4, 6, 8) surfaces after exposure to a 30‰ salinity, filtered seawater suspension of *Amphora coffeaeformis* (10^5 cells per mL) for 24 h.

as is also indicated by the XPS wide-scan spectra of polymer-coated SS surfaces (Fig. 2). Since the fluorescence images can only provide a visual comparison of the effect of the polymer-coated SS surfaces on *Amphora* adhesion, it is important to quantify the adhered *Amphora* cells.

Several methods, including recording the *in vivo* chlorophyll autofluorescence of *Amphora* cells on an *in situ* surface[44] and counting the *Amphora* cells in a captured fluorescence image,[54] have been used to detect and quantify *Amphora* cells adhered to surfaces. Inspired by the bacterial quantification method, involving ultrasonic cell removal, serial dilution and plating for viable cell counts,[55] a technique for measuring the fluorescence intensity of ultrasonically removed *Amphora* cells from the surface has been developed. The autofluorescence of chlorophyll in *Amphora* cells exhibits a major emission peak centered at about 690 nm at an excitation wavelength (λ_{ex}) of 440 nm (Fig. S4†). The emission maximum at 690 nm was selected for the subsequent fluorescence intensity recording. Prior to the surface detachment of *Amphora* cells, the ultrasonic stability of chlorophyll autofluorescence was measured. Fig. S5† shows the fluorescence intensity evolution of *Amphora* cells at 690 nm as a function of sonication time. The fluorescence intensity of *Amphora* cells increase insignificantly ($P > 0.05$) with the increase in sonication time and reach a plateau after about 6 min, suggesting that the ultrasonic treatment has only limited effect on the fluorescence intensity of *Amphora* cells. The enhancement in fluorescence intensity may have been caused by the better dispersion of *Amphora* cells upon ultrasonic treatment. Thus, the ultrasonic treatment on *Amphora* cells can be applied for the subsequent study. To explore the feasibility of this technique, the ultrasonic detachment of *Amphora* cells from SS surface was also studied by fluorescence microscopy. Fig. S6† shows the fluorescence images of *Amphora* cells on the pristine SS surfaces before and after ultrasonic treatment. Almost all of the *Amphora* cells have been removed from the pristine SS surface after sonication for 10 min. This result confirms that the *Amphora* cells on the SS surface can be effectively dislodged by sonication.

The combination of ultrasonic cell removal and chlorophyll autofluorescence detection is used to quantify the adhesion of *Amphora* cells on the SS surfaces. The fluorescence intensity of *Amphora* cells at 690 nm *versus* the cell number exhibits a linear relationship (Fig. S7†). Thus, the chlorophyll fluorescence intensity ratios of the polymer-coated to the pristine SS surface can reflect the ratios of cell number on these surfaces. Fig. 6 shows the quantitative assay of *Amphora* adhesion on the pristine and polymer-coated SS surfaces. In comparison to the pristine SS surface, the SS-P(DMA-*co*-PEGMEMA) and SS-(PEI/P(DMA-*co*-PEGMEMA))$_n$ (n = 2, 4, 6, 8, 10) surfaces reduce *Amphora* adhesion to ~60%, 34%, 32%, 28%, 21% and 21%, respectively. The SS-P(DMA-*co*-PEGMEMA) surface is more susceptible to *Amphora* adhesion compared to the SS-(PEI/P(DMA-*co*-PEGMEMA))$_n$ (n = 2, 4, 6, 8, 10) surfaces. This phenomenon is consistent with the trend observed qualitatively from fluorescence microscopy investigation (Fig. 5).

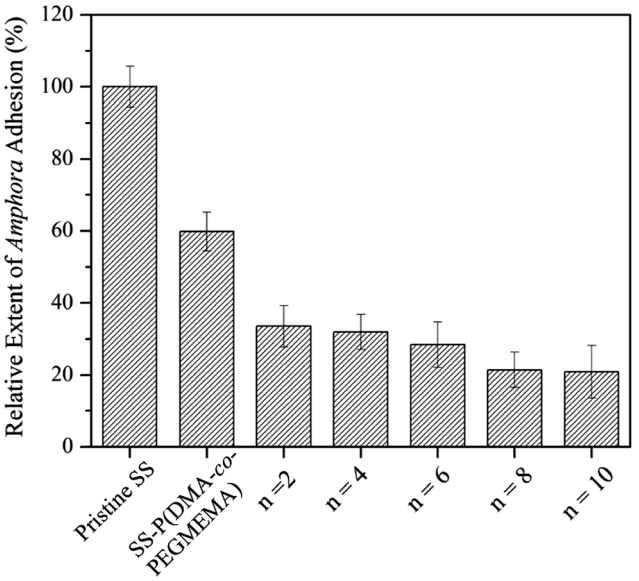

Fig. 6 Relative extent of *Amphora* adhesion on the pristine SS, SS-P(DMA-*co*-PEGMEMA) and SS-(PEI/P(DMA-*co*-PEGMEMA))$_n$ surfaces after exposure to a 30‰ salinity, filtered seawater suspension of *Amphora coffeaeformis* (10^5 cells per mL) for 24 h. Error bars give the standard deviation obtained from three replicates.

Barnacle cyprid settlement on the SS-(PEI/P(DMA-*co*-PEGMEMA))$_n$ substrates

Barnacles are probably the most problematic macrofoulers with a wide geographical distribution.[45,56,57] The cyprid from adult barnacles (*Balanus amphitrite*) was selected for the investigation of *in vitro* antifouling effects of the polymer-coated SS surfaces under static conditions. Fig. 7 shows the percentage of settled and dead cyprids on the pristine and polymer-coated SS surfaces after an exposure time of 24 h. About 65% of the

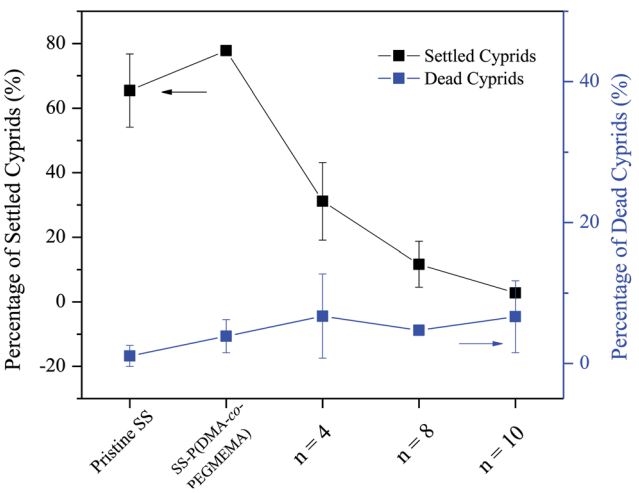

Fig. 7 Percentage of settled and dead barnacle cyprids on the pristine SS, SS-P(DMA-*co*-PEGMEMA) and SS-(PEI/P(DMA-*co*-PEGMEMA))$_n$ surfaces relative to the total population of approximately 40 cyprids, after 24 h of settlement assay. Error bars give the standard deviation obtained from three replicates.

barnacle cyprids settle on the pristine SS surface. PEG-modified surfaces are known to exhibit fouling resistance to barnacle cyprids.[51] The hydrated PEG-based polymer coatings probably also weaken the adhesion of glycoproteins secreted by the cyprids in order to cement themselves on the surface. However, the settlement of barnacle cyprids does not decrease accordingly, after the anchroing of P(DMA-*co*-PEGMEMA) monolayer onto the SS surface (SS-P(DMA-*co*-PEGMEMA)). This phenomenon is probably due to the monolayer coverage of P(DMA-*co*-PEGMEMA) with insufficient hydration to resist the settlement of barnacle cyprids. LBL deposition of PEI/P(DMA-*co*-PEGMEMA) bilayers significantly reduces the settlement of barnacle cyprids. The percentage of settled barnacle cyprids on the SS-(PEI/P(DMA-*co*-PEGMEMA))$_n$ ($n = 4$, 8, 10) decrease with the increase in the number of bilayers. These results suggest that the thickness of the polymeric antifouling coatings is critical to the settlement of macrofoulers. The dead fractions of cyprids, after in contact with the polymer-coated SS surfaces for 24 h, are between 4% and 7%, which are comparable to that of the pristine SS surface. These results translate into very low or negligible toxicity for the polymer-coated SS surfaces.

Conclusions

Stainless steel surfaces were modified by LBL-assembly of the catechol-containing and fouling-resistant P(DMA-*co*-PEGMEMA) layer and amino-rich PEI layer *via* spontaneous catechol-amine reaction to improve their stability and integrity. The PEI/P(DMA-*co*-PEGMEMA) bilayers-coated SS surfaces can effectively inhibit the adhesion of marine bacteria and microalgae (microfouling), as well as settlement of barnacle cyprids (macrofouling). In comparison to the existing metal-based self-polishing or biocide-embedded polymer coatings, the PEI/P(DMA-*co*-PEGMEMA) multilayer coatings provide an environmentally-friendly alternative to inhibition of marine fouling. The LBL assembly by catechol-amine reaction can be readily extended to the functionalization of many other metal and metal oxide substrates, which are known to interact with catechols. This LBL technique can also be extended to other catechol-containing synthesized and natural polymers. The synthesized polymers can be fluorine-rich and hydrophobic, quaternary ammonium-functionalized and antimicrobial, or zwitterionic and low-fouling, while the natural polymers can be agarose, chitosan or alginate.

Acknowledgements

The authors would like to acknowledge the financial support of this study from the A*STAR-SERC MIMO Program under Grant no. 1123004048 (NUS WBS no. R279-000-356-305).

References

1 C. Jullien, T. Bénézech, B. Carpentier, V. Lebret and C. Faille, *J. Food Eng.*, 2003, **56**, 77–87.
2 K. A. Whitehead, P. S. Benson and J. Verran, *Biofouling*, 2011, **27**, 907–917.
3 H. Hermawan, Introduction to Metallic Biomaterials, in *Biodegradable Metals*, Springer, Berlin, Heidelberg, 2012.
4 R. Pilliar, Metallic Biomaterials, in *Biomedical Materials*, ed. R. Narayan, Springer, US, 2009.
5 J. Landoulsi, K. E. Cooksey and V. Dupres, *Biofouling*, 2011, **27**, 1105–1124.
6 M. Stach, Z. Kroneková, P. Kasák, J. Kollár, M. Pentrák, M. Mičušík, D. Chorvát Jr, T. S. Nunney and I. Lacík, *Appl. Surf. Sci.*, 2011, **257**, 10795–10801.
7 Q. Zhao and Y. Liu, *J. Food Eng.*, 2006, **72**, 266–272.
8 W. J. Yang, T. Cai, K. G. Neoh, E. T. Kang, G. H. Dickinson, S. L. M. Teo and D. Rittschof, *Langmuir*, 2011, **27**, 7065–7076.
9 L. J. Bastarrachea and J. M. Goddard, *J. Appl. Polym. Sci.*, 2013, **127**, 821–831.
10 M. Ignatova, S. Voccia, B. Gilbert, N. Markova, D. Cossement, R. Gouttebaron, R. Jérôme and C. Jérôme, *Langmuir*, 2005, **22**, 255–262.
11 Y. Iwasaki, A. Matsumoto and S. I. Yusa, *ACS Appl. Mater. Interfaces*, 2012, **4**, 3254–3260.
12 Y. Yang, C. Poleunis, L. Románszki, J. Telegdi and C. C. Dupont-Gillain, *Biofouling*, 2013, **29**, 1123–1137.
13 R. Rosmaninho, O. Santos, T. Nylander, M. Paulsson, M. Beuf, T. Benezech, S. Yiantsios, N. Andritsos, A. Karabelas, G. Rizzo, H. Müller-Steinhagen and L. F. Melo, *J. Food Eng.*, 2007, **80**, 1176–1187.
14 S. Pavlukhina and S. Sukhishvili, *Adv. Drug Delivery Rev.*, 2011, **63**, 822–836.
15 Z. Tang, Y. Wang, P. Podsiadlo and N. A. Kotov, *Adv. Mater.*, 2006, **18**, 3203–3224.
16 Y. Li, X. Wang and J. Sun, *Chem. Soc. Rev.*, 2012, **41**, 5998–6009.
17 P. Bertrand, A. Jonas, A. Laschewsky and R. Legras, *Macromol. Rapid Commun.*, 2000, **21**, 319–348.
18 F. Caruso, *Adv. Mater.*, 2001, **13**, 11–22.
19 E. Kharlampieva, V. A. Izumrudov and S. A. Sukhishvili, *Macromolecules*, 2007, **40**, 3663–3668.
20 F. Wang, N. Ma, Q. Chen, W. Wang and L. Wang, *Langmuir*, 2007, **23**, 9540–9542.
21 I. Erel-Unal and S. A. Sukhishvili, *Macromolecules*, 2008, **41**, 8737–8744.
22 I. Suzuki, Y. Egawa, Y. Mizukawa, T. Hoshi and J. I. Anzai, *Chem. Commun.*, 2002, 164–165.
23 O. Roling, C. Wendeln, U. Kauscher, P. Seelheim, H. J. Galla and B. J. Ravoo, *Langmuir*, 2013, **29**, 10174–10182.
24 Y. Shimazaki, M. Mitsuishi, S. Ito and M. Yamamoto, *Langmuir*, 1997, **13**, 1385–1387.
25 Y. Yu, H. Zhang, C. Zhang and S. Cui, *Chem. Commun.*, 2011, **47**, 929–931.
26 P. Schuetz and F. Caruso, *Adv. Funct. Mater.*, 2003, **13**, 929–937.
27 J. Langecker, H. Ritter, A. Fichini, P. Rupper, M. Faller and B. Hanselmann, *ACS Appl. Mater. Interfaces*, 2012, **4**, 619–627.
28 K. M. Gattás-Asfura and C. L. Stabler, *ACS Appl. Mater. Interfaces*, 2013, **5**, 9964–9974.
29 S. Y. Yang and M. F. Rubner, *J. Am. Chem. Soc.*, 2002, **124**, 2100–2101.

30 J. Sun, T. Wu, Y. Sun, Z. Wang, J. C. Zhang, X. Shen and W. Cao, *Chem. Commun.*, 1998, 1853–1854.
31 G. K. Such, J. F. Quinn, A. Quinn, E. Tjipto and F. Caruso, *J. Am. Chem. Soc.*, 2006, **128**, 9318–9319.
32 W. J. Yang, D. Pranantyo, K. G. Neoh, E. T. Kang, S. L. M. Teo and D. Rittschof, *Biomacromolecules*, 2012, **13**, 2769–2780.
33 L. A. Connal, C. R. Kinnane, A. N. Zelikin and F. Caruso, *Chem. Mater.*, 2009, **21**, 576–578.
34 M. E. Buck, J. Zhang and D. M. Lynn, *Adv. Mater.*, 2007, **19**, 3951–3955.
35 A. H. Broderick, U. Manna and D. M. Lynn, *Chem. Mater.*, 2012, **24**, 1786–1795.
36 J. Seo, P. Schattling, T. Lang, F. Jochum, K. Nilles, P. Theato and K. Char, *Langmuir*, 2009, **26**, 1830–1836.
37 J. Wu, L. Zhang, Y. Wang, Y. Long, H. Gao, X. Zhang, N. Zhao, Y. Cai and J. Xu, *Langmuir*, 2011, **27**, 13684–13691.
38 H. Lee, Y. Lee, A. R. Statz, J. Rho, T. G. Park and P. B. Messersmith, *Adv. Mater.*, 2008, **20**, 1619–1623.
39 Y. Min and P. T. Hammond, *Chem. Mater.*, 2011, **23**, 5349–5357.
40 E. Faure, C. Falentin-Daudré, T. S. Lanero, C. Vreuls, G. Zocchi, C. Van De Weerdt, J. Martial, C. Jérôme, A. S. Duwez and C. Detrembleur, *Adv. Funct. Mater.*, 2012, **22**, 5271–5282.
41 M. Eberhardt, R. Mruk, R. Zentel and P. Theato, *Eur. Polym. J.*, 2005, **41**, 1569–1575.
42 F. D. Jochum, L. Zur Borg, P. J. Roth and P. Theato, *Macromolecules*, 2009, **42**, 7854–7862.
43 S. J. Yuan and S. O. Pehkonen, *Colloids Surf., B*, 2007, **59**, 87–99.
44 K. Rasmussen and K. Ostgaard, *Biofouling*, 2000, **15**, 275–286.
45 B. H. Tan, H. Hussain, K. C. Chaw, G. H. Dickinson, C. S. Gudipati, W. R. Birch, S. L. M. Teo, C. He, Y. Liu and T. P. Davis, *Polym. Chem.*, 2010, **1**, 276–279.
46 K. Nilles and P. Theato, *J. Polym. Sci., Part A: Polym. Chem.*, 2010, **48**, 3683–3692.
47 L. Q. Xu, J. C. Chen, R. Wang, K. G. Neoh, E. T. Kang and G. D. Fu, *RSC Adv.*, 2013, **3**, 25204–25214.
48 P. Glass, H. Chung, N. R. Washburn and M. Sitti, *Langmuir*, 2009, **25**, 6607–6612.
49 K. L. Tan, L. L. Woon, H. K. Wong, E. T. Kang and K. G. Neoh, *Macromolecules*, 1993, **26**, 2832–2836.
50 P. K. Jha and G. P. Halada, *Chem. Cent. J.*, 2011, **5**, 1–7.
51 D. Pranantyo, L. Q. Xu, K. G. Neoh, E. T. Kang, W. Yang and S. L. M. Teo, *J. Mater. Chem. B*, 2014, **2**, 398–408.
52 M. Li, K. G. Neoh, L. Q. Xu, R. Wang, E. T. Kang, T. Lau, D. P. Olszyna and E. Chiong, *Langmuir*, 2012, **28**, 16408–16422.
53 A. F. Wu, K. Nakanishi, K. L. Cho and R. Lamb, *Biointerphases*, 2013, **8**, 1–10.
54 X. Y. Zhu, D. Janczewski, S. S. C. Lee, S. L. M. Teo and G. J. Vancso, *ACS Appl. Mater. Interfaces*, 2013, **5**, 5961–5968.
55 Z. Shi, K. G. Neoh, E. T. Kang and W. Wang, *Biomaterials*, 2006, **27**, 2440–2449.
56 I. Y. Phang, K. C. Chaw, S. S. H. Choo, R. K. C. Kang, S. S. C. Lee, W. R. Birch, S. L. M. Teo and G. J. Vancso, *Biofouling*, 2009, **25**, 139–147.
57 N. Aldred and A. S. Clare, *Biofouling*, 2008, **24**, 351–363.